An introduction to low dose electron tomography- from specimen preparation to data collection

G. Rh. Owen[1,*] and **D.L.Stokes** [1,2]

[1]New York Structural Biology Center, 89 Convent Avenue, New York, NY-10027, USA.
[2]Skirball Institute of Biomolecular Medicine, Department of Cell Biology, New York University School of Medicine, New York, NY 10016, USA

Keywords: electron tomography; low dose electron microscopy; high pressure freezing; plunge freezing

1. Introduction

Electron tomography is a technique that uses a Transmission Electron Microscope (TEM) to determine a three-dimensional (3D) structure from any given asymmetric object [1]. This process can be simply broken down into 3 steps. First, a series of two dimension projection images of the specimen are recorded and systematically tilted to different angles in the microscope. Second, these individual images are aligned to a common origin. Finally, the projections are then backprojected to create a 3D representation of the sample [2].

Modern commercial instruments now provide a computerized interface, which has been exploited to develop software for automated data collection of the tilt series. As a result, electron tomography is growing in popularity. Before attempting to collect data for tomography it is important to note that the resolution of the data will depend on specimen preparation, imaging conditions and image processing. In this review we attempt to address two of the important issues in electron tomography namely biological specimen preparation and imaging conditions. The reader is directed to Frank 2006 [3] for a comprehensive overview of the current data processing methods.

2. Sample preparation

Electron microscopes use electrons for imaging the sample. Electrons interact very strongly with matter and the column of the electron microscope must have a high vacuum to prevent extraneous scattering. Furthermore, the sample must be very thin to allow sufficient numbers of electrons to pass through and form an image. Native biological samples are incompatible with a vacuum because of their high water content and therefore need to be dehydrated before imaging in an electron microscope. Thus, the first goal of standard biological sample preparation (known as chemical fixation) is to preserve the native structure of the biological specimen during dehydration. Chemical fixation is generally used for this purpose, but is limited in its ability to preserve the fine structure. One problem is the slow action of conventional fixatives due in part to their slow diffusion into biological tissues. As a result, fixed tissue often reflects the specimen's response to the fixative rather than the living state. A detailed discussion on the chemical fixation mechanisms is described by Hayat (2000) [4].

For high-resolution work, there is a need to maintain the position of the cell constituents during fixation at a scale that is finer than the desired resolution. Clearly, chemical fixation is not suitable for this situation because if its dependency on slow diffusion.

Cryo-fixation is a method that exploits the high content of water in biological material and uses it as a fixative. Contrary to chemical fixation this physical method is fast and does not change the state of the specimen and has the potential to preserve biological structures at the atomic level. However, to

* Corresponding author: e-mail: gowen@nysbc.org, phone: ++1 212 939 0660

understand cryo-fixation the physical properties of water and its role in the biological specimen should be understood.

2.1 Role of water in the cell

Living organisms contain a large volume of water (approximately 70%). This water associates with all molecules within the organism. As a consequence of this interaction the surfaces of nearly all biological macromolecules, macromolecular assemblies and biological membranes are hydrophilic. This hydrophilicity is governed by the nature of the chemical groups at the surfaces of these structures which are capable of forming transient hydrogen bonds with water that form a "hydration shell" and prevents molecules from aggregating. More importantly the hydration shell is involved in the conformation of biological macromolecules (proteins for instance), as the macromolecule is orientated according to how the water interacts to the charges on its surface [5].

During the process of chemical fixation proteins are crosslinked, so that they can withstand the aggregation tendency upon removal of their hydration shell by the organic solvent during a subsequent dehydration step. Since water removal is the limitation in ultrastrucutral preservation, using the water as the fixative is a logical step. Cryofixation is a method of stabilizing water in the hydration shell by rapidly lowering the temperature below freezing point to make a solid. Depending on the temperature and pressure solid water can exist in at least 9 different stable crystalline forms, one metastable crystalline form and one or two metastable amorphous forms. In cryofixation there are three forms of ice that are of interest: 1) Amorphous ice known as the non-crystalline vitreous state; 2) Hexagonal ice (most energetically favorable structural arrangement of water) and 3) cubic ice (metastable form of ice encountered only when amorphous ice is heated in the range between 193K and 123K. In cryofixation we seek the vitreous state in order to obtain the best possible preservation of the sample, *i.e.* without altering the native distribution of water molecules in the sample. Hexagonal ice on the other hand will nucleate and form crystals. These crystals will grow and cause segregation and damage to elements of the sample.

There are five ways in which to obtain amorphous or vitrified ice in biological samples. These are freezing point depression (adding antifreeze which may affect the osmotic balance in the sample); undercooling (270K-250K is the limit in most biological systems); rapid cooling (heat is removed faster than ice crystal formation); small samples (they lose heat faster than larger samples); low temperature storage (to prevent cubic ice formation). In his section we focus on two cryofixation methods: High pressure freezing (which utilizes freezing point depression, rapid cooling and low temperature storage to freeze large specimens) and plunge freezing (which utilizes rapid cooling of small samples followed by low temperature storage).

2.2 High Pressure Freezing (HPF)

The principles of HPF are based on the fact that crystallisation of water is limited to the temperature zone between the melting point and the vitrification temperature [6]. For pure water this zone is between 273K to approximately 140K. In physiologically active cells and tissues it is between 271K and 193K, reflecting their decreased water activity. By using the principle of Le Chatelier (that freezing increases water volume and that high pressure inhibits such expansion) it is only logical that high pressure will hinder crystallization. A decrease in crystallisation also requires less heat extraction per unit time of cooling because crystallisation is an endothermic process. In practice the HPF device subjects the samples to pressure of 2045 bar, which decreases the melting temperature of water to a minimum of 251K [7]; within a few milli seconds, a jet of liquid nitrogen cools the sample to below the vitrification temperature. During this process, the sample is protected in a sandwich-like aluminum holder known as "Hats" or planchets. Any unoccupied space between the specimen and the surface of the hat is filled with 1-hexadecene (hydrophobic solution) providing an uncompressible liquid in air space that would otherwise collapse [8]. The pressure is transduced to the sample through a small gap between the two

hats and the hat surface on either side of the specimen is exposed to cooling (Fig. 1). This simultaneous double sided cooling theoretically will successfully vitrify a 600µm thick specimen, though a 300µm thickness is a more realistic goal in the field.

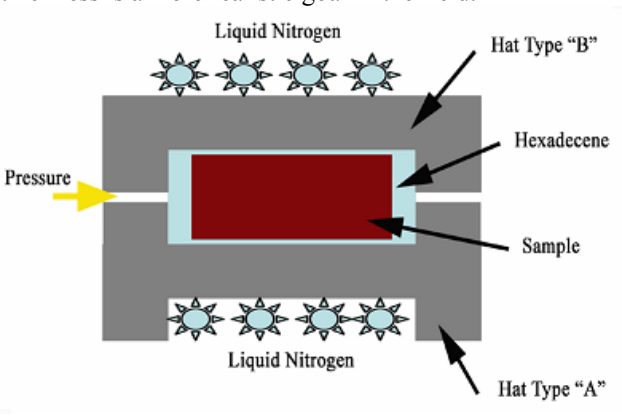

Figure 1. Schematic representation of a cross-section through a sample sandwiched between aluminum hats for high pressure freezing. The free space between the sample and the hat is filled with Hexadecene. Pressure is transduced to the specimen through the space between the two hats. Rapid cooling of the specimen occurs first by an increase in pressure immediately followed by jets of liquid nitrogen projected onto opposite sides of the specimen.

2.3 Plunge Freezing

In the case of HPF the conditions are adapted to vitrify thick samples. For plunge freezing the sample thickness has to be more limited. Thus, this technique is used mainly for small protein assemblies that are in suspension. Also known as an immersion cryofixation method, a few microliters of the aqueous suspension are placed onto a glow discharged (negatively charged) holey carbon grid. Protein assemblies are generally attracted to the negatively charged surface, and some suspension will span the holes of the carbon. Excess suspension is blotted with filter paper, leaving a very thin (100-200 nm) layer of liquid, which is plunged at ~1m/s into the cryogen (Fig. 2).

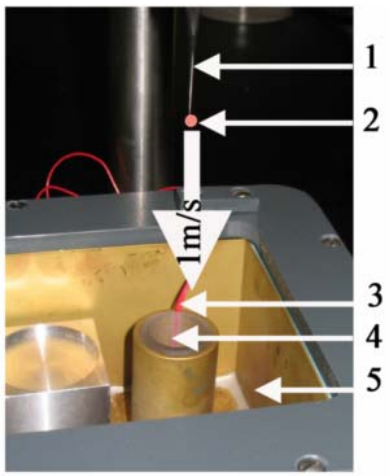

Figure 2. A typical apparatus setup for plunge freezing. Fine tweezers (1) fixed onto an injector rod grips a grid with a drop of sample solution placed upon its negatively charged holey carbon coating. This drop is blotted with filter paper before plunging the sample at a speed of 1m/s into liquid nitrogen (5) cooled liquid ethane (4). The liquid ethane is kept at melting temperature by a heater surrounding the liquid ethane chamber (3).

Many liquified gases (such as liquid nitrogen) are not appropriate as cryogens for plunge freezing because they envelop any warmer object with a thermally insulating layer of gas (Leidenfrost Effect). For optimal results the primary cryogen is used to cool a secondary cryogen with a better cooling rate. Ethane has the best cooling rate of any liquefied gases (mean cooling rate 13-15 x 10^3 Ks^{-1}). It also has the advantage of having a high vapour pressure at low temperatures, which allows ethane residues present on the sample to be easily eliminated from the vitrified specimen before observation. Although the technique is quite simple to master there are a few technical constraints to keep in mind:
1) The secondary cryogen must be kept at a temperature that is above its freezing point, but below the vitrification temperature of the sample. The melting temperature of the secondary cryogen can be

maintained by installing a heater around the chamber containing the cryogen. 2) Once the sample has been blotted with filter paper the thin aqueous suspension can evaporate very quickly. Therefore, the surrounding environment must be maintained with high humidity (above 60%). 3) The sample must be held at a temperature above freezing (so that the sample is not frozen) before plunging. As a precaution the sample should be at least a few cm above the cryogen to avoid being frozen in the cold gas. 4) It is important that the sample moves through the cryogen while it is freezing to maximize forced convective cooling (the most efficient heat transfer method). The path length can be calculated so that the sample is at the same temperature as the cryogen by the time it comes to rest.

Plunge freezing is a very convenient and fast way for cryofixation. The apparatus is quite easy to build and holey carbon grids of known hole diameters and distribution are commercially available (Quantifoil Micro Tools GmbH, Jena, Germany). Although homemade plunging devices have been routinely used to good effect, a robotically controlled version (Vitrobot™, FEI, Eindhoven, The Netherlands) is available and claims to have better sample reproducibility because the procedure is computer controlled and the chamber is controlled for temperature and humidity.

It should be noted that two other methods of rapid freezing not covered in this review are propane jet freezing and freeze slamming. These are typically used with tissue samples and fall somewhere between HPF and plunge freezing in their efficiency.

2.4 Sample preparation for imaging

Once the samples have been preserved by cryofixation, the ultimate goal is to image them with the electron microscope. Because blotting of aqueous suspensions is effective in creating a sufficiently thin sample prior to plunge freezing, the corresponding samples can be directly imaged in the frozen state by loading them onto a cryoholder, which uses liquid nitrogen to maintain the sample in its vitreous state while inside the electron microscope. For thicker specimens frozen by HPF, sections in the order of 100 nm must be cut to enable the transmission of sufficient numbers of electrons to create an image. Cryoultramicrotomy can produce such ultrathin sections directly from the frozen tissue; these are usually mounted onto grids and directly imaged in the frozen state with a cryoholder. For more information on this topic the reader is referred to Marko *et al*., 2006 [9]. Electron tomographic reconstruction of frozen hydrated sections has great potential but presently the technique is limited to specialized groups dedicated to this technique. One significant problem is getting the sections to lie flat on the specimen support. A very low success rate in producing suitable samples represents a serious bottleneck in applying the technically demanding, but generally manageable, imaging protocol required for tomography. A promising development is the use of focused ion beam technology to create thin areas from a block of frozen tissue. This alternative method to sectioning might be the way to avoid the practical difficulties of cryoultramicrotomy and handling of the resulting frozen-hydrated sections.

Conventional methods for sectioning biological tissue involves chemical fixation, dehydration, embedding in an epoxy resin and sectioning by ultramicrotomy. After polymerization, the epoxy resin provides a supporting matrix with optimal mechanical characteristics for sectioning; furthermore, this resin has proven to be resilient to electron beam irradiation. Such sections have a consistent physical state and thickness, making this method ideal for creating electron tomography samples. One limitation of epoxy resin embedding is that it can only be done at room temperature and that the resins are immiscible with water. Dehydration causes the most damage to the tissue, such that molecular structures are not generally preserved and strong fixation is required to maintain the general morphology of membranes and cell organelles. Water miscible acrylic resins have been developed [10] so that the whole procedure of infiltration and polymerisiation can be done at low temperature, but acrylic resins are not as resilient to electron beam irradiation, are negatively affected by electron dense fixatives, and produce irreproducible section quality. An alternative to these problems involves substituting ice with another solvent that does not crystallize as the sample is warmed up to room temperature after cryofixation. This technique is called freeze substitution and is based on slowly substituting the ice in a sample while

gradually increasing the temperature. Thus, the tissue is fully dehydrated before reaching room temperature, at which point it can be embedded in epoxy resin at room temperature [11].

2.5 Freeze substitution (FS)

Freeze substitution is a technique whereby the bulk water and hydration shell are removed by an organic liquid carried out at a temperature low enough to maintain a vitreous state of water and avoid secondary ice-crystal growth. Once this is accomplished the temperature can be raised to room temperature since no ice crystals will form when water is absent [12]. Bulk water removal is facilitated by the fact that it is not strongly bound to any macromolecules and occurs at 193K. Upon further dehydration as the temperature is raised to 233K and 243K, the hydration shell is removed and consequent changes to the conformation of molecules [13].

The lowest temperature for successful FS is at the melting point of the organic solvent used. On the other hand, there is danger of tissue damage by secondary ice crystal growth at temperatures higher than the devitrification range of amorphous ice, which is 190K. Therefore any solvent with a melting temperature that is lower than 190K is ideally suited for FS. Not all solvents that have melting temperature within this range are suitable for FS. The dehydration of the sample depends also on the water capacity of the solvent. Both methanol (melting temp 179.1K) and acetone (177.6K) are used as FS solvents but have very different water capacity. At 193K, acetone can substitute approximately 2.5% water but its substitution rate is dramatically reduced while methanol can absorb 10% without affecting the substitution rate, which is fairly rapid. If acetone is to be used as a substitution medium then it is recommended that the volume is a thousand times greater than the sample volume [14].

The preservation of the hydration shell at 193K but removing the bulk water is the goal of FS. Non-polar solvents are ideal for preserving the hydration shell. Such solvents are used in experiments where the principal objective is to retain the original location of water soluble substances rather than preserve ultrastructural detail, and include diethyl ether. Polar solvents such as methanol will substitute bulk water and function in the presence of high amounts of water. Dipolar solvents such as acetone are now widely used for general morphology of cryofixed tissues. Dipolar solvents cause less lipid extraction [15] but have the disadvantage that they must be relatively water free before substitution.

The extraction of the hydration shell and solutes by these harsh organic solvents as the temperature is raised from 193K to 273K can be prevented by the addition of chemical fixatives to the substitution media. The type of fixative is limited by its solubility therefore water-soluble only fixatives are out of the question. Since acetone is regarded as the solvent of choice for substitution this makes adding fixatives such as uranyl acetate (insoluble in acetone) or water containing aldehydes difficult without introducing water to the solvent system. Fortunately uranyl acetate can be pre-dissolved in methanol then added in a concentrated solution to acetone without the significant addition of water. Osmium tetroxide, a fixative as well as being very electron dense, is soluble in either methanol or acetone, which makes it very suitable for FS. Osmium tetroxide is volatile at room temperature and rapidly dissolves in solvents. It should therefore be prepared fresh and cooled immediately to the substitution temperature. Presently there is some evidence that the addition of a small amount of water in the substitution medium (1%) can improve membrane visualization [16].

Chemical fixative reactivities at low temperatures are largely unknown. White *et al.,* (1976) [17] suggested that osmium tetroxide might react with double bonds of unsaturated fatty acids at a temperature as low as 200K. Humbel (1984) [18] found that uranyl acetate reduced the extraction of phospholipids from 9% to 2% at 203K and from 15% to 4% at 243K. Humbel *et al.,* 1983 [19] showed that glutaraldehyde could also crosslink bovine serum albumin at temperatures as low as 223K but at a much reduced rate compared to higher temperatures. Since reactivity of fixatives are limited by their ability to diffuse throughout the tissue, there is a need to provide a prolonged incubation time to ensure complete fixation. Most FS protocols however are stepwise to provide a longer water substitution time at low temperature where the fixatives are ineffective, followed by increasing the temperature to allow fixative crosslinking. A typical fixation method used for mouse neonatal skin [20] can be seen in Table

1. Acetone was used as the substitution media with the addition of osmium tetroxide and uranyl acetate. This substitution duration is rather long and Muller *et al.,* 1980 [11] has suggested 8 hours per step as being sufficient. The authors believe that there is a need to empirically determine the times that are optimal for any given sample, but this protocol is a good starting point.

Table 1. A typical freeze substitution protocol.

Temperature (K)	Substitution Time (h)	Process Occurring	Warm up rate (K per h)
183	48	Water substitution	278
213	24	Fixation/ Water substitution	278
243	18	Fixation/ Water substitution	278
273	0.1	Rinse with fresh acetone x3 to remove fixative	-
293	Approx. 1	-	-

2.6 Assessing sample preservation quality

Assessing the quality of cryofixation is important before proceeding to tomography. In the case of plunge freezing this is rather simple. First of all if the ice surrounding the sample is too thick then the electron beam will not penetrate and consequently no beam will be visible. If however the electron beam does penetrate the ice, then a quick and easy way of determining ice thickness is by the density of the ice. A light shade of grey is normally a good indication that the ice is thin enough and acceptable for imaging. A more quantitative approach is to use the electron beam to burn a hole through the ice. The density measured in this hole should be 20-40% higher than the surrounding ice and can be estimated using the automatic exposure reading from the microscope. The type of ice can be assessed only electron diffraction. Vitrified ice produces a broad diffraction ring at ~0.37 nm in the electron diffraction pattern indicating the liquid-like distribution of water molecules. For cubic ice, this broad ringed pattern becomes a sharp ringed pattern, reflecting the presence of small crystallites at various different orientations. Hexagonal ice crystals are generally larger and therefore produce sharp diffraction spots at characteristic spacings corresponding to the underlying crystal lattice [23].

After HPF followed by FS it is not possible to distinguish between vitreous ice and hexagonal ice with electron diffraction as the ice has been substituted by an organic solvent. Segregation of cellular ultrastructure is one indication of ice damage. A more definitive indicator of ice crystal damage is the presence of small holes or clear spaces in the cytoplasm. These spaces will be surrounded by electron dense fibrillar material which represents precipitates of cellular material (Fig. 3a). Ice crystallization will also cause rupturing of the cell membranes and this is most apparent in the mitochondria. However, it is the nucleus that is the intracellular organelle most susceptible to ice-crystal damage. If chromatin is compact and dense, sharply delineated and clearly contrasted the state of preservation is optimal. In ice damaged samples the nuclear chromatin appears honeycombed in organisation.

2.7 Ultramicrotomy

In HPF samples, the entire block of tissue is not necessarily preserved to the same extent. External surfaces generally experience faster freezing rates and are therefore better preserved than the middle of the block. Therefore, sectioning the sample where optimal freezing has occurred can save valuable sectioning time. For example in a 600μm thick piece of skin, knowing the depth of freezing on each side of the sample will allow you to focus on areas that are likely to have been optimally frozen. One can expect good freezing at a depth of 100-150μm from the surface of the HPF hat. However, freezing results are often unpredictable and it is worth sampling several areas of a block before concluding that it has been ruined by ice crystal damage. After forming a ribbon of grey section (>60nm) it is important to

place the sections across the centre of the grid. Having the sections along the tilt axis will facilitate the automated data collection system. The samples are now ready for tomography.

3. Low dose Electron Microscopy

When imaging a biological specimen preserved either in vitreous ice or epoxy resin the irradiation of these samples with electrons can damage the specimen. With so much emphasis on limiting any changes to the specimen during the preservation techniques the goal of low dose microscopy is to minimize the electron dose on the specimen while maximizing the signal to noise ratio in the resulting images.

3.1 Electron specimen Interaction

Electrons interact with the specimen in two different ways. Elastic collisions with the specimen occur when the electrons are deflected without energy loss as they pass through the specimen. These electrons are appropriately focused by the lenses in the electron microscope and therefore provide high-resolution information; since these electrons impart little energy to the specimen, they cause virtually no radiation damage. During inelastic collisions, energy is transferred from the electron to the specimen. The amount of energy lost depends on the specimen's chemical composition and the exact nature of the collision.

3.2 Irradiation and its effect on the sample

The effects of irradiation on the sample include radiation damage (caused by the ionizing effect of the beam) and thermal damage (energy absorbed by the specimen and is dissipated as heat). The amount of energy absorbed by the specimen is dependent on the accelerating voltage and the number of incident electrons. Specimen damage decreases with increasing accelerating voltage (the faster the electrons travel the lower the cross-section for scattering) and lower beam currents (fewer electrons interacting with the specimen reduce the number of inelastic scattering events). Current TEM's for cryo microscopy are typically armed with a 200-300 KeV gun and produce a more coherent electron beam due to their field emission source. The higher accelerating voltages provide better optics and allow thicker specimens to be imaged and the beam coherency greatly improves the resolution that can be derived from a given image.

For frozen samples, it is important to maintain the specimen at low temperature. Typically, cryoholders will maintain specimen temperatures below 100K, where phase changes (vitreous to cubic) to the ice should be small. To ensure their proper function, however, it is important to establish good thermal contact between the grid and the cryoholder [21]. The total electron dose applied to the specimen must be carefully controlled to avoid radiation damage. One readily observable change to the sample that the user will see is bubbling (Fig. 3b). The extent of bubbling depends on the density and size of the organic sample and this will generally occur at a cumulative dose of 4000-8000 electrons/nm^2. However, more subtle effects occur at much lower doses, where high resolution features are lost. Therefore, when recording single projection images for high resolution image processing for single particle analysis or two-dimensional crystallography, the dose is generally limited to 1200-2000 electrons/nm^2. On the other hand, when recording of an entire tilt series for tomographic reconstruction, a higher dose will be used to maximize the signal-to-noise ratio in the three-dimensional reconstruction.

Changes to the sample with irradiation are not only constrained to cryo samples. Although stained, embedded samples are extremely resilient to the electron beam changes do occur with these samples also. An excellent review by Egerton *et al*., 2006 [23] provides comprehensive details on all aspects of electron beam effects on biological samples. Many of the effects of the beam, as described above, also occur with embedded plastic sections. Most notably is the formation of free radicals and ions that cause bond scission and molecular chain scission. Further exposure can cause damage to secondary structures and tertiary reorganization. One especially important effect is the loss of specific groups and altered structural composition that will undoubtedly cause mass loss and hence specimen shrinkage. Indeed, it is

common to apply a pre-irradiation to stained, embedded sections prior to collecting tilt series to ensure that specimen shrinkage has stabilized to a relatively constant level [24]. Some samples however are more resilient to shrinkage. Densely packed proteins such as the cadherins of the desmosome show this quality [20].

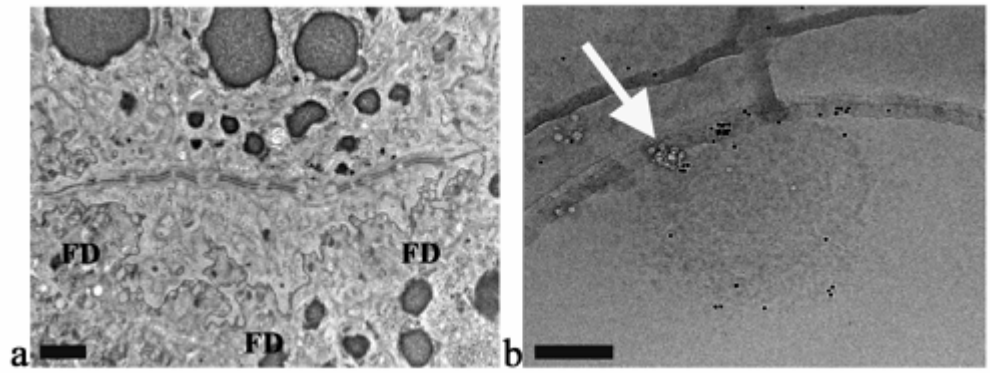

Figure 3. Electron micrographs displaying freeze damage and the effect of irradiation on a specimen embedded in vitreous ice. (a) Ultrathin resin section of neonatal mouse skin having undergone high pressure freezing followed by freeze substitution. The boundary between two cells can be determined by the cell-cell desmosome adhesions between them. A front of freeze damage (FD) by ice crystal formation is visible in the lower cell. Grid bar 1μm (b) Bubbling can be seen (arrow) within an isolated desmosome embedded in ice. This is the result of over irradiating the cryo sample and is a process that depends on the size and density of the organic sample. Determining the maximum dose the sample can withstand is advisable before preparing for tilt series acquisition. Grid bar = 100nm.

Limiting and controlling the amount of sample irradiation is the goal of low dose electron microscopy. Because the greatest sample irradiation occurs during image set up such as searching and focusing this method involves performing these steps away from the area of interest. In this case searching is done at very low magnification at low exposure (or using a defocused electron diffraction image for lower dose and higher contrast) and the focusing is performed at high magnification to one side of the area of interest (Fig. 4). In particular, for focusing tilted samples the beam is shifted under computer control along the tilt axis to ensure that the focus is determined at the same height as the area of interest.

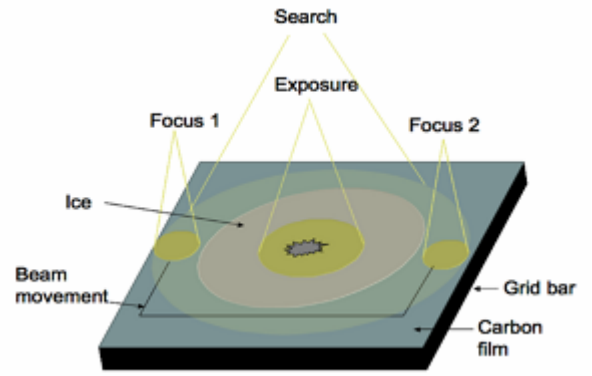

Figure 4. Simplified representation of low-dose image acquisition. Irradiation of the sample is restricted only for image acquisition. Searching the sample is done at low magnification utilizing the CCD camera sensitivity to display suitable imaging areas. Rather than focusing on the sample the beam shifts away from the sample and returns to the predetermined spot for image acquisition.

4. Low dose Electron Tomography

Electron tomography is a technique that utilizes the TEM's large depth of field to study samples from 50-500nm in thickness (from whole cells to suspension of macromolecular complexes). The resolution of the resulting tomogram will depend on the specimen preparation, microscope conditions and image

processing but is usually between 5 and 10nm. The theoretical resolution can be determined by the tilt angle increments $\Delta\alpha$ and for linear tilt increments d is given by the relationship [25]:

$d = \pi D/N$

where : D = diameter of the spherical object
N = number of projections recorded at equally spaced tilt angles over a range of 180^o.

This equation is only valid if the geometrical thickness of the specimen is independent of the tilt angle and if the sample can be tilted over a full 180º angle. Neither criteria is practical on a routine basis. As the tilt angle increases the specimen thickness increases (with $1/\cos\alpha$), and tilt angles are usually limited to -70^o to 70^o because of the specimen holder mechanical constraints and bars from the specimen support obscuring the field of view.

Conceptualizing the sampling of 3D data is difficult. One way to represent the image data is in Fourier space. Fourier transforms decompose the image into its sine and cosine components. The output image of the transformation represents the image in the Fourier space while the input image is the real space equivalent. When only $-70^o/+70^o$ tilt range is possible providing 140^o of specimen information in Fourier space this missing information is referred to as the missing wedge (Fig. 5). To reduce the effects of the missing wedge it is possible to use dual-axis tomography [26,27], which decreases the missing area into a pyramid. In any case, data normal to the electron beam (corresponding to 90º tilt angle) is missing and, as a result, tomograms will have anisotropic resolution [28].

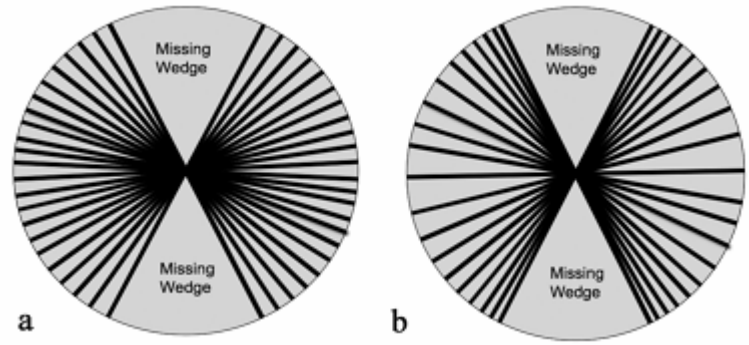

Figure 5. Schematic representation of limitation of data collection if the sample is not fully tilted -90o/+90. The resulting loss of data is represented by the "missing wedge" (a). The specimen can be more efficiently sampled at higher tilt angles using the Saxton tilt increment scheme (b). In addition to the missing wedge information will be lost depending on the tilt increments used.

4.1 Imaging conditions

In tomography the specimen thickness has to be sufficiently thin to provide a projection image of the specimen but not so thick that it obscures beam penetration at high tilt angles. In thin samples electrons transverse the specimen and undergo inelastic or elastic scatter events as described above. Phase contrast is generated by 90º phase shifts between elastically scattered electrons and the unscattered electron beam. Amplitude contrast is generally quite small (5-10%) and results in a diminution in the amplitude of scattered waves relative to unscattered ones. Both phase and amplitude contrast are capable of providing high resolution information in the images. Aperture contrast results from electrons that are scattered at high angle so that they fall outside the objective aperture and is effective in defining the outline of features, especially in stained samples where the high atomic number of stain produces very strong scattering. Inelastic scattering results in a blurred image that detracts from the image quality. Above certain specimen thicknesses, the fractions of inelastic and scattered electrons become too high, thus masking the high-resolution information. Successful imaging of the specimen invariably depends on choosing an appropriate specimen thickness and dose rate to provide a signal to noise ratio that is high

enough to produce a meaningful image. Using high accelerating voltages can be effective in increasing the signal to noise ratio, especially for thicker specimens. If higher accelerating voltage microscopes are not available energy filtering techniques can be used to enhance image contrast by removing part of the inelastic electron component.

The allowable cumulative electron dose tolerated for a frozen, unstained sample is 0.4-0.8 e/nm^2. For the tilt series required for electron tomography, this dose must be partitioned between the many images taken at various tilt angles. For imaging vitrified isolated desmosomes the authors used a dose of 0.5 e/nm^2 at 200KeV for 100 tilt increments between -70/+70. In order to minimize the number of images one can use the so-called Saxton scheme [29], where the tilt increment depends on the cosine of the overall tilt angle. Thus, tilt increments are larger at low tilts and smaller at high tilts. This scheme provides an even sampling in Fourier space and optimal partitioning of dose into a minimum number of images. Although CCD cameras are available with 4096x4096 pixels, their point spread functions are such that it is sensible to bin these images two-fold to 2048x2048. This increases signal to noise ratio and does not substantially degrade the resolution. Using an objective aperture produces useful contrast in the image, but the aperture size should be large enough so that it does not obscure the beam during as a result of image shifts applied during acquisition of the tilt series. Increasing the defocus is also useful in enhancing the image contrast. In particular, a defocus >5μm will generate substantial phase contrast that will aid in subsequent image alignment and tomogram interpretation. Ultimately, this defocus should be chosen such that the first zero of the Contrast Transfer Function (CTF) matches the target resolution for observing structural information (Fig.6).

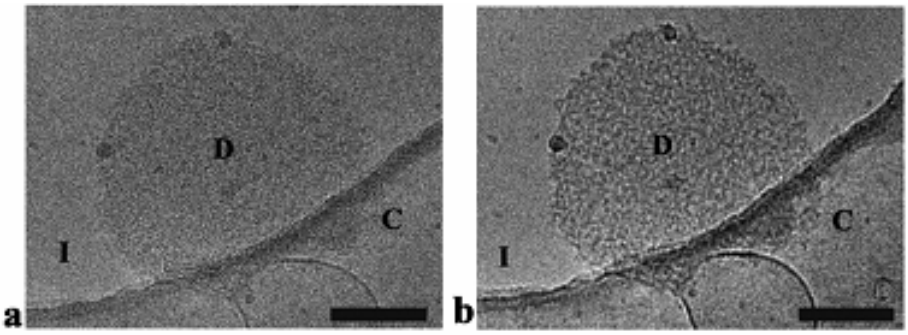

Figure 6. Increasing the phase contrast of isolated desmosome (D) embedded in vitreous ice (I) in a holy carbon film (C) by increasing the defocus value from 4μm to 12μm. Grid bar 100nm.

4.2 Tomography automation

It is quite clear that radiation sensitivity of the sample is one of the main problems for data collection in tomography. Other parameters during data collection at different tilt angles pose many problems especially during the tomogram reconstruction step. Manually collecting images at various tilt angles is a tedious procedure and is prone to failure since the goniometer imperfections causes lateral movement of the specimen during tilting. These movements will add up to a micron or more in the best case and will cause problems during tomogram reconstruction: *e.g.*, focus changes will limit image resolution and lateral displacement will limit the common area present in the entire tilt series. Computer control of the image acquisition process automatically corrects the image shifts and focus changes during acquisition of the tilt series. These procedures also minimize the electron dose on the sample during these adjustments. Automatic focusing compares two images acquired at opposite beam tilts to determine the defocus and this procedure is done on an area adjacent to the object of interest; accuracy for such focus determinations tend to be high (approximately 5nm for thin samples) [30]. In the first generation software, specimen displacements were measured at each new tilt angle by comparisons with images taken at the previous tilt angle. Each image required steps for search, track, focus then exposure until the full angular tilt range was covered. To compensate for the shift the current in the image shift coils were

changed so that the image of interest remained centered. More recent methods have tried to make the acquisition process accurate and faster. The pre-calibration system capitalizes on the reproducibility of the goniometer during the tilt series. A calibration curve is recorded in advance using the same specimen holder so that image shifts and defocus values can be changed without having to record all the requisite images [31]. The pre-calibration method is limited to the FEI range of microscopes. Another automated acquisition method known as the prediction method can be used with any microscope and is currently available as freeware (Serial EM- http://bio3d.colorado.edu/SerialEM –[32]). This system models the changes in image shifts and focus changes at the first few tilt angles to predict image movements for the remainder of the tilt series. By assuming that the sample follows a certain geometric rotation, the optical system characterizes the offset between the optical and mechanical axes so image movement in the x,y, and z directions due to stage tilt can be dynamically predicted with high accuracy. The main advantage of this system is that it does not need tracking and focusing once the system is set up. Full tomogram acquisition at 2^o tilt increments using the Saxton scheme, resulting in ~100 images in the final tilt series, can be completed in 1h, which makes it possible to collect many tilt series in a given session on the microscope.

Conclusion

Tomograms are a very elegant way of displaying ultrastructure in 3D. In this review we have tried to inform the reader that before beginning any data collection understanding the preparation processes and the imaging conditions used will have a huge impact on the interpretation of the data. For further information regarding the calculation and interpretation of the tomographic structures, we refer the reader to works by Frank 2006 [2].

References

[1] D. De Rosier and A. Klug, Nature **217**,130 (1968).
[2] J. Frank, Electron Tomography, Springer, New York, 2006.
[3] J. Frank, Three-dimensional electron microscopy of macromolecular assemblies. Oxford University Press 2006.
[4] M.A. Hayat, Principles and Techniques of Electron Microscopy. Cambridge University Press 2000.
[5] M.A. Lauffer, Entropy Driven Processes in biology, Springer, New York (1975).
[6] H. Moor, G. Bellin, C. Sandri and K. Akert, Cell Tissue Research **209**, 201 (1980).
[7] H. Kanno, R.J. Speedy and C.A. Angell, Science **189**, 880 (1975).
[8] D. Struder, M. Michel and M. Muller, Scanning Microscopy Supplement **3**, 253 (1989).
[9] M. Marko, C. Hsieh and C.A. Mannella, Electron Tomography, Springer, New York, 2005, pp 49-82
[10] E. Kellenberger, E. Carlemalm, W. Villiger, J. Roth and R.M. Garavito, Low Denaturation Embedding for electron microscopy of thin sections. Chemische Werke G.m.b.H. Wladkraiburg.1980.
[11] M. Müller, Marti T, and Kris S, Proceedings of the 7th European Congress of electron Microscopy, Leiden 1980, pp 720-721.
[12] R.M.K.W. Lee, A critical appraisal of the effects of fixation, dehydration and embedding on cell volume, In Revel J-P, Barnard T, and Haggis GH (eds) The Science of biological specimen preparation, SEM, AMF O'Hare, Chicago, pp 165-174 (1984).
[13] H. Gross, High-resolution metal replication of freeze-dried specimens in Cryotechniques in biological electron Microscopy ed. RA Steinbrecht & K Zierlold, 1987, pp.205-215.
[14] R.A. Steinbrecht and M. Müller , Freeze substitution and freeze drying in Cryotechniques in biological electron Microscopy ed. RA Steinbrecht & K Zierlold, 1987, pp.149-168.
[15] C. Weibull, W.Villiger, and E. Carlemalm, Journal of Microscopy **134**, 213 (1984).
[16] P. Walther and A. Zeigler, Journal of Microscopy **208**, 3 (2000).
[17] D.L. White, S.B. Andrews, J.W. Faller and R.J. Barnet, Biochim Biophys Acta **436**, 577 (1976).
[18] B.M. Humbel, Gefriersubstitution – Ein Weg zur Verbesserung der morphologischen und zytochemischen Untersuchung biologischer proben im electronmikroskop., Diss, Eidgen Tech Hochschule Zurich (1984).
[19] B.M. Humbel, T. Marti, and M. Müller, Beitr Electronenmikrosk Direktabb Oberfl **16**, 585(1983).
[20] W. He, P. Cowin and D.L. Stokes, Science **302**,109 (2003)
[21] J. Dubochet, J. Lepault, R. Freeman, J.A. Berriman and J.C. Homo, Journal of Microscopy**128**, 219 (1982).
[22] Y.Talmon and E.L.Thomas, Journal of Microscopy **111**, 151 (1977).

[23] R.F. Egerton, P. Li and M. Malac, Micron **35**, 399 (2004).
[24] P.K. Luther, M.C. Lawrence and R.A. Crowther, Ultramicroscopy **24**, 7 (1988).
[25] R.A. Crowther, L.A. Amos, J.T. Finch, D.J. De Rosier, A. Klug, Nature **226**, 421 (1970).
[26] D.N. Mastronarde, Journal of Structural Biology **120**, 343 (1997).
[27] P. Penczek, M. Marko, K. Buttle and J. Frank, Ultramicroscopy **3**, 393 (1995).
[28] W. Baumeister and A.C. Steven, Trends in biochemical sciences **25**, 624 (2000).
[29] W.O. Saxton, W. Baumeister and M. Hahn, Ultramicroscopy **13**, 57 (1984).
[30] A.J. Koster, A. van der Bos, K.D. van der Mast, Ultramicroscopy **21**, 209 (1987).
[31] U. Ziese, A.H. Janssen, J.L. Murk, W.J. Geerts, T. Van der Krift, A.J. Verkleij and A.J. Koster, Journal of Microscopy **205**, 187 (2002).
[32] D.N. Mastronarde, Journal of Structural Biology **152**, 36 (2005).